Journal of Materials and Environmental Sciences
ISSN : 2028-2508

JMES, 2017 Volume 8, Issue 8, Page 3138-3150

http://www.jmaterenvironsci.com/

Interfacial Electrochemical Properties of a Moroccan Bentonite in aqueous suspension

Abderrahim El Mragui, Ikram Daou, Rachid Chfaira and Omar Zegaoui*

Research Team: Materials and Applied Catalysis, Moulay Ismaïl University, Faculty of Sciences; BP. 11201 Zitoun, Meknes, Morocco

Received 23 Dec 2016,
Revised 25 Feb 2017,
Accepted 28 Feb 2017

Keywords

- ✓ Moroccan bentonite;
- ✓ Potentiometric titration;
- ✓ Conductometric titration;
- ✓ Complexation constant;
- ✓ Ionisation constant ;
- ✓ pH_{pzc}

Omar Zegaoui:
o.zegaoui@fs.umi.ac.ma
+212 6 61 07 06 66

Abstract

In this work, the interfacial electrochemical properties of a purified Moroccan bentonite have been studied. The conductometric studies showed that the bentonite particles were stable in aqueous phase in the studied pH range (3-12). The potentiometric titration results obtained in the presence of various concentrations of non-specifically adsorbed electrolytes showed that the point of zero charge shifted to lower pH values by increasing electrolyte concentrations. This behavior was attributed to the combined effect of both variable charges and structural negative charges. The adsorption sequence's study carried out at various ionic strengths showed that the bentonite particles in aqueous phase behave as a water structure organizer at pH below to pH_{pzc}, while at pH range superior to pH_{pzc} they behave as a water structure disorganizer. The total number of surface sites, determined by using the graphical extrapolation method, was 7.4 OH/nm^2. Based on the obtained values of the complexation constants, it was concluded that the adsorption of non-specifically ions (Li^+, Na^+, Cl^- and Br^-) was exclusively electrostatic whereas that of specifically ions (Cs^+ and F^-) was both electrostatic and specific nature.

1. Introduction

During the past few years, natural aluminosilicate minerals (e.g. clay minerals) have received a great interest in industrial and environmental chemistry because of their abundance, important physicochemical and adsorptive properties (high surface area, large cation exchange capacity, high chemical and mechanical stability,…) [1]. These properties confer them high sorption ability, even for the heavy organic molecules [1]. Bentonite is widely used as an adsorbent material to remove metals [2,3], organic molecules [4], pesticides [5] and radionuclides [6]. Natural Bentonite, which is inexpensive and environmental friendly material, is abundant and exists in several deposits around the world, particularly in the Northeast of Morocco [7]. Bentonite, which is predominantly montmorillonite, is dioctahedral clay of smectite group and is composed of stacked interconnected sheets containing one sheet of alumina octahedral (O) (Al^{3+} in octahedral coordination with O^{2-}) sandwiched between two sheets of silica tetrahedra (T) (Si^{4+} in tetrahedral coordination with O^{2-}) [8]. The interconnection is ensured by the sharing of O^{2-} at polyhedral corners and edges leading to a T-O-T composition [9,10]. An isomorphic substitution within the octahedral sheets (Al^{3+} by Mg^{2+} and/or Fe^{2+}/Fe^{3+}) and tetrahedral sheets (Si^{4+} by Al^{3+}) can occur in natural clays. Because of this substitution, the surface of the T-O-T layers becomes negatively charged and the interlayers are occupied by exchangeable cations (Na^+, Ca^{2+}, K^+) to neutralize the excess of charge [10]. The adsorptive properties of clay minerals are closely related to their interfacial electrochemical properties that are a result of interactions between electrically charged particles and molecules of solvent. It has been reported that montmorillonite particles carry two kinds of electrical charges [11-13]. The first one is variable and depends on the pH of the solution, and results from the adsorption/desorption reactions on surface hydroxyl groups. These hydroxyl groups originating from broken and hydrolyzed Al-O and Si-O bonds are located at the edge surface of the particles [11,14]. The second one is negative and is caused by the isomorphic substitution in the octahedral alumina layer [13,15]. They are the main responsible of the electrical, sorptive, and coagulative properties of the bentonite minerals [15]. Several investigations have been carried out to study the adsorption of ions on montmorillonite [16-21]. They showed that montmorillonite displays a particular acid-base behavior in which no

common intersection point between the titration curves at different ionic strengths was observed [16-18,20,21]. In their study concerning the adsorption of H^+ on Argentinean Na^+-montmorillonite, Avena *et al.* [17] reported the presence of structural negative charges in the clay particle, and variable charge sites and cation exchange sites at the surface. Leroy *et al.* [19] have proposed an electrochemical model to describe the electrochemical properties of clay minerals and colloidal suspensions of the mineral surface. Their model included a speciation model of the active crystallographic surface sites plus a classical description of the Stern and diffuses layers. The use of the surface titration of minerals in aqueous electrolyte solutions is one way to investigate the sorptive and electrical behavior of minerals. The data are generally collected from acid-base potentiomentric and conductometric titrations [17,22-30]. The main goal of this work is to study the interfacial electrochemical properties of a natural Moroccan bentonite by using acid-base potentiometric and conductometric titrations at 25°C. These properties concerned the determination of the insolubility state of the dispersed phase in the dispersing phase, the point of zero charge (pH_{pzc}), the total number of surface sites (Ns), the action's nature of the dispersed phase on the dispersing phase, and the surface ionization and complexation constants. The adsorption studies were carried out in the presence of various ions such as Li^+, Na^+, Cs^+, F^-, Cl^- and Br^-.

2. Materials and Methods

2.1. Materials

The natural bentonite used in this work was taken from a deposit in the Northeast of Morocco (region of Nador). The bentonite sample was purified by sedimentation following the experimental procedure described previously [31]. As reported in our previous work [31], the chemical composition of the bentonite sample determined by X-Ray Fluorescence (XRF) analysis (Table 1) indicated the presence of large amounts of silica and alumina while Fe_2O_3 and MgO were present in the solid with less amounts. It has been suggested that some of Fe^{3+} and Mg^{2+} cations replaced Al^{3+} cations in octahedral sites [31]. The exchangeable interlayer cations (Na^+, Ca^{2+} and K^+) as well as other oxides existed in the form of traces in the solid. The obtained cation exchange capacity and specific surface area for this clay were 88.82 $meq/_{100}g$ and 74.02 m^2/g, respectively [31].

Table 1: Chemical composition, surface area and CEC of the bentonite sample

Sample	Chemical composition (wt%)
SiO_2	54.80
Al_2O_3	18.00
Fe_2O_3	6.00
MgO	5.12
Na_2O	1.75
CaO	0.35
K_2O	0.25
OO [a]	3.53
LI [b]	10.20
Total	100
CEC [c] ($meq/_{100}g$)	88.82
S_{BET} [d] (m^2/g)	74.02

a: Other oxides in trace
b: Loss on ignition at 900°C
c: Cation exchange capacity determined by using a method based on cobaltihexamine chloride absorbance [31].
d: Specific surface area determined by N_2 adsorption at -196°C according to the standard Brunauer-Emmett-Teller [31].

As reported in our previous work [31], the X-Ray Diffraction (XRD) results showed that the bentonite sample was constituted almost exclusively of montmorillonite phase in addition to traces of quartz and cristobalite. The alkali-halide electrolytes NaCl (99.9 %), CsCl (99.9 %), NaF (99.5%), NaBr (99.5 %) and LiCl (99.9 %) used in this work were of analytical grade and supplied by Sigma Aldrich Company. In all experiments, the used distilled water was filtered through a column of mixed resin such a way that its specific conductivity was of 0.510^{-6} ($\Omega^{-1}.cm^{-1}$).

2.2. Potentiometric and conductometric titrations

2.2.1. Experimental device

Potentiometric and conductometric titrations were performed at 25°C using the same experimental device able to measure a surface charge of a solid with a volume fraction of minimal specific surface area of 5 m^2/g. All electrolyte solutions were freshly used. Before acid-base titration experiments were started, an aqueous suspension (100 ± 1 mL) containing 0.5 g of bentonite was stirred for 20 hours to establish the equilibrium of the ionic exchange between the dispersing and dispersed phases. Figure 1 shows the evolution of pH according to the contact time between bentonite and aqueous solution. A slower equilibration is observed, and about 10 hours were required for equilibrating the bentonite dispersion. Analogous results were observed by Avena *et al.* [17] with an Argentinean montmorillonite. They explained this behavior, among others, by the edge-to-face interactions between positively charged edges and negatively charged faces.

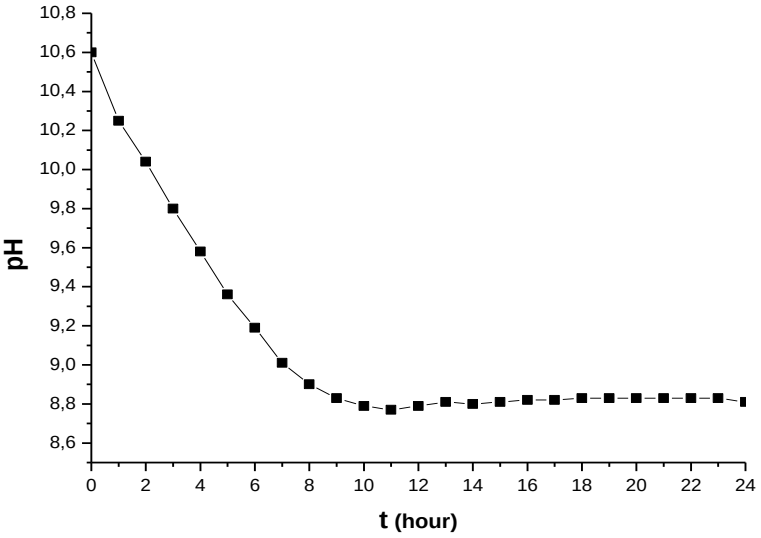

Figure 1: Evolution of pH with contact time of dispersing and dispersed phases

2.2.2. Determination of the surface charge density

It has been reported that when immersed in aqueous solutions, natural clays develop surface charges that originate from the clay and from other species naturally contained in clays [30,32]. The surface charge density is a result of the unequal potential adsorption of H^+ and OH^- [23]. The experimental data of the surface charges were obtained by potentiometric titrations of aqueous suspensions containing a fixed concentration of an electrolyte [22] in the presence and the absence of bentonite.

The experimental acid-base titration procedure was as follows: 100 ± 1 mL of a blank solution or aqueous bentonite suspension was introduced in a thermostatic bath adjusted at 25±1 °C. The blank solution was constituted of an aqueous solution containing a fixed concentration of an electrolyte (i.e. 10^{-2} mol/L of NaBr) and 0.5 mL of HCl at 0.494 mol/L. The aqueous bentonite suspension was identical to the blank solution in which 5 g/L of bentonite were added. The homogenization of the suspension was provided by using a mechanical stirrer motor equipped with a propeller stirrer. The titrant solution (0.2 mol/L of NaOH) was added as 50 ±0.005 µL increments after no pH and specific conductivity were observed (about 15 min). The titration experiments were stopped when the pH was around 12. In all cases, the titrant additions were performed with a micropipette, and the pH and conductivity were measured with a pH meter Type Microcomputer pH/mV/TEMP METER 6171 and a conductometer Type Inolab cond 730, respectively. Figure 2 shows an example of the obtained acid-base potentiometric titration curves for the blank solution and the aqueous suspension containing 5 g/L of bentonite.

The surface charge density σ_0 was calculated by comparing the titration curves obtained for the blank solution and the aqueous solution containing 5 g/L of bentonite.

σ_0 can be calculated by using the following equation:

$$\sigma_0 = \frac{\sum N_{Av} . n_i . q_i}{S} \qquad \text{(eq.1)}$$

where : $q_i = Z_i.e$ (e =1,602.10^{-19} C), S the surface of the solid, n_i the mole number of H^+ and OH^-, N_{Av} the Avogadro constant.

$\sigma_0 = \frac{\sum_i n_i.N_{Av}.Z_i.e}{S} = \sum_i F.Z_i.\Gamma_i$ (eq.2)

where $F = N_{Av}.e$ is the Faraday constant and $\Gamma_i = \frac{n_i}{S}$ the analytical excess of the surface ion "i"

Since H^+ and OH^- are the ions determining the potential hence,

$\sigma_0 = F(\Gamma_{H^+} - \Gamma_{OH^-})$ (eq.3)

- if $\Gamma_{OH^-} < \Gamma_{H^+}$ ➔ $\sigma_0 > 0$: the H^+ surface ions are in excess with respect to OH^- ions.
- if $\Gamma_{OH^-} > \Gamma_{H^+}$ ➔ $\sigma_0 < 0$: the OH^- surface ions are in excess with respect to H^+ ions.
- if $\Gamma_{OH^-} = \Gamma_{H^+}$ ➔ $\sigma_0 = 0$: corresponds to the pH of the point of zero charge.

The Eq. 2 expressing σ_0 becomes:

$\sigma_0 = \frac{\sum n_i.N_{Av}.Z_i.e}{S} = \frac{F.n_{eq}}{S}$ (eq.4)

where $n_{eq} = n_i.Z_i$;

The specific surface area of the solid is $A = \frac{S}{m_s}$ (m^2/g), where m_s is the mass of the solid (g) and S its surface (m^2).

$\sigma_0 = \frac{F.}{A.}.\frac{n_{eq}}{m_s}$ (C/m^2) (eq.5)

$|Z_{H^+}| = |Z_{OH^-}| = 1$

$n_{eq} = n_i = C_B\ .\Delta V.10^{-6}$

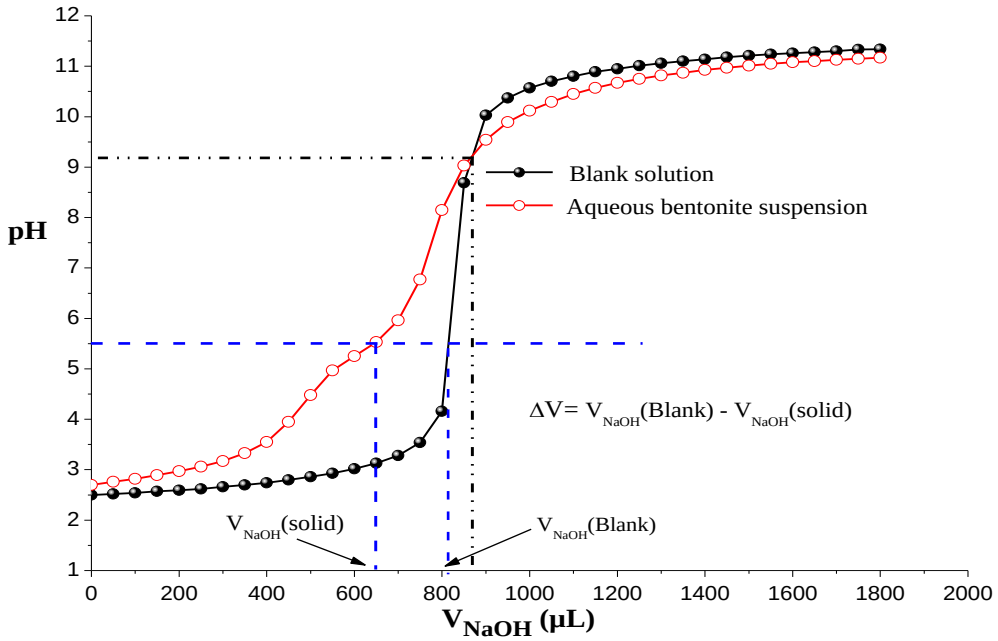

Figure 2: Acid-base potentiometric titrations for the blank solution and the aqueous suspension containing 5 g/L of bentonite.

For a fixed pH value, $\Delta V = V_{NaOH}(blank) - V_{NaOH}(solid)$ (µL) (see Figure 2)

C_B is the concentration of the titrant (NaOH)

$\sigma_0 = \frac{10^6.F.C_B.\Delta V.10^{-6}}{10^4.A.m_s} = 10^{-4}.\frac{F.C_B}{A.m_s}.\Delta V$ ($\mu C/cm^2$) (eq.6)

For each oxide and at a fixed concentration of the titrant, $10^{-4}.\frac{F.C_B}{A.m_s} = Cst$ and σ_0 depends on the pH of the colloidal solution

$\sigma_0 = Cste\ .\ \Delta V$ (eq.7)

In this work, C_B= 0.2 mol/L, m_s=0.5 g, A=74 m^2/g and the Cst = 0.05216.

Figure 3 shows the obtained curve corresponding to σ_0 according to the pH. It was deduced from Figure 2 data by using a Matlab language program developed in our laboratory.

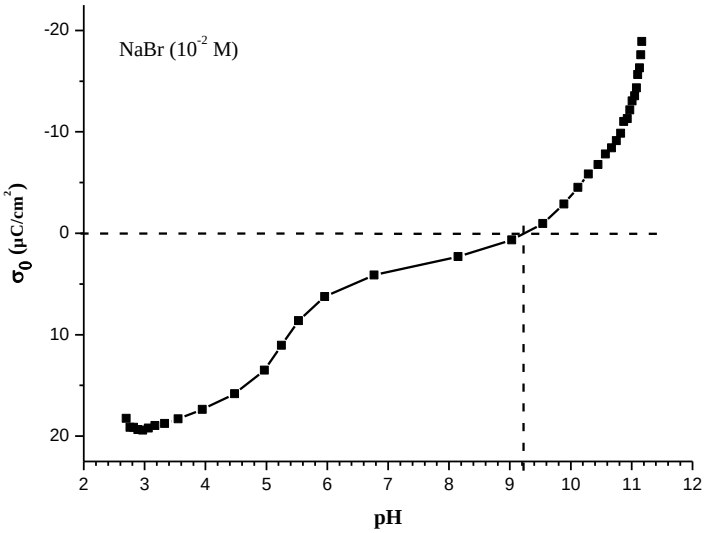

Figure 3: σ_0 vs pH curve deduced from acid-base potentiometric titrations presented in Figure 2.

3. Results and discussions

3.1. Solubility of bentonite particles in dispersing phase

For a colloidal sol, such as natural bentonite in aqueous suspension, the determination of the interfacial electrochemical properties requires the preliminary identification of the insolubility domains of the dispersant phase in the dispersing phase. This study was carried out by using conductometric titrations according to the pH. The principle of these measurements was based on the comparison of two types of conductometric titration curves (Figure 4). The first ones are recorded for the blank titrations of aqueous solutions containing various electrolytes (LiCl, NaCl, CsCl, NaBr and NaF) and 0.5 mL of HCl (0.494 mol/L). The second curves concern the conductometric titrations recorded, in the same experimental conditions, in the presence of bentonite (5 g/L) [33]. At a given pH, the difference in specific conductivity between the two recorded conductometric titrations curves corresponds to the conductivity provided both by the determinant ions of the potential (H^+ and OH^-) and the soluble ionic species provided from the solubility of the particles in the dispersing phase. Figure 4 shows examples of specific conductometric titration curves obtained for blank aqueous solutions and aqueous bentonite suspension in the presence of 10^{-3} M of LiCl (minimum solubility corresponding to a non-specific adsorption : Figure 4A) and 10^{-1} M of CsCl (maximum solubility corresponding to a specific adsorption: Figure 4B). From these figures, we can observe that the difference in conductivity depends on the nature and the ionic strength of the used electrolyte. So, the solubility of the studied bentonite in the dispersing phase depends on the nature and the ionic strength of the used electrolyte. From Figures 4A and 4B, it can be observed that the differences between the specific conductivity recorded for blank solutions (χ_{Blank}) and that of aqueous bentonite suspensions ($\chi_{bentonite}$) range from 40 to 170 µS/cm, indicating a low concentration of soluble species from bentonite. So, it can be concluded that the studied bentonite sample can be considered stable in aqueous phase in the studied pH range.

3.2. The point of zero charge pH (pH_{pzc}). Effect of the ionic strength

One of the most important parameters used to describe the surface properties of variable charge of minerals is the point of zero charge (PZC). This point corresponds to the pH at which the net total particle surface charge density is zero (pH_{pzc}) [34,35]. This is also the pH at which the total net particle charge density (σ_0) equals to zero. A mineral carries a net negative charge if the solution pH is greater than its PZC and a net positive charge occurs at pH values lower than the PZC [35,36]. Several methods can be used to determine experimentally the point of zero charge of a colloidal suspension. They generally rely on ion adsorption, potentiometric titration or electrophoretic mobility measurements [37-42]. The traditional experimental approaches use acid-base potentiometric titrations. In this case, the pH_{pzc} can be obtained from the acid-base potentiometric titration curves σ_0 vs pH. It corresponds to the pH where titration curves cross with those of the corresponding blank solutions. The potentiometric titration curves involve also the measurement of the point of zero salt effect (PZSE), corresponding to the pH at which salt concentration has no effect on the adsorption of ions [35]. The σ_0 vs pH curves plotted for various concentrations of an electrolyte intersect at this point. Figure 5 shows an example of potentiometric titration

curves σ_0 vs pH obtained, in this work, in the presence of various concentrations of a non-specifically adsorbed electrolyte (NaBr) and bentonite (5 g/L). Two important conclusions can be drawn from the analysis of these curves. *1)* The σ_0 vs pH titration curves didn't display a clear common intersection point in the studied pH range.

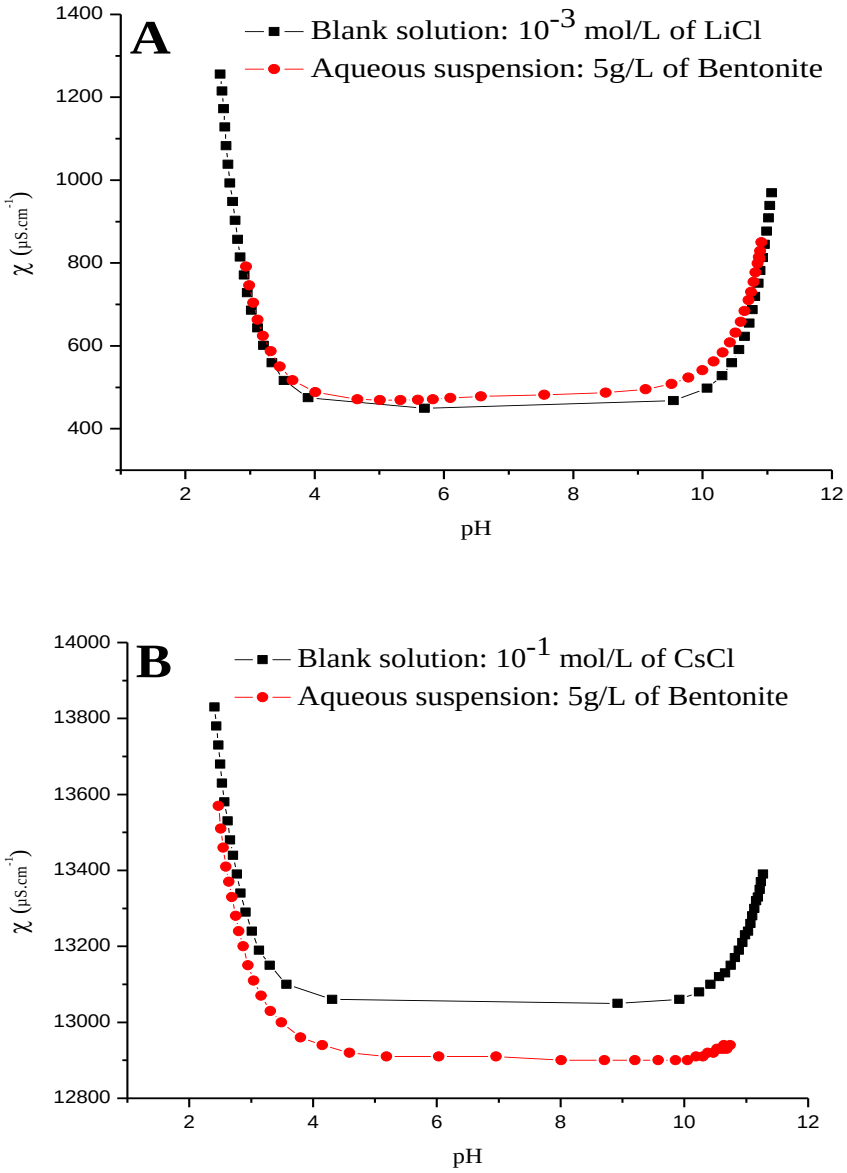

Figure 4: Specific conductometric titration curves obtained for blank aqueous solution and aqueous suspension containing 5 g/L of bentonite in the presence of 10^{-3} M of LiCl (A) and 10^{-1} M of CsCl (B).

This behavior has been observed also by many authors for the titration curves of 2:1 clays [17,26,27,30]. Some theoretical studies [43-45] have explained this behavior by the direct or indirect effects of the structural charge on the dissociation of the edge sites. *2)* The point of zero charge shifted to lower pH values by increasing electrolyte concentrations. Their values were 9.29, 9.24 and 8.79 for titrations performed at 10^{-1}, 10^{-2} and 10^{-3} mol/L of NaBr, respectively (Figure 5). These results were in good agreement with those reported by many authors [17,46-51] for other montmorillonite and clay samples carrying structural negative charge as the main behavior source of charge and potential. This behavior that is not exhibited by simple oxides has been attributed to the combined effect of both variable charges and structural negative charges. It is noteworthy that this behavior reveals the studied particles carry a net negative charge at the point of zero charge.

However, for a specific adsorption of an electrolyte, Figures 6 and 7 show examples of potentiometric titration curves σ_0 vs pH obtained in the presence of bentonite, and various ionic strengths of a specifically adsorbed CsCl and NaF, respectively. Figure 6 shows that the pH_{pzc} shifted towards the lowest pH values when the ionic strength

of CsCl was increased from 10^{-3} to 10^{-1} mol/L, indicating that CsCl is indifferent to the HCl existing in the solution. In contrast, Figure 7 shows that the pH_{pzc} shifted towards the highest pH values when the ionic strength of NaF was increased. On the other hand, the σ_0 vs pH potentiometric titration curve obtained for NaF at 10^{-3} mol/L (Figure 7) shows that F^- was specifically adsorbed but NaF was indifferent to HCl present in the solution. The titration equations can be expressed as follows:

$HCl + NaF \rightarrow HCl + NaF$ (I)

$HCl + NaF + NaOH \rightarrow H_2O + NaF + NaCl$ (II)

At NaF ionic strength superior to 10^{-3}mol/L, the obtained σ_0 vs pH potentiometric titration curves (curves corresponding to C_{NaF} = 10^{-2} and 10^{-1}mol/L, Figure 7) indicate that F^- was adsorbed but NaF was no longer indifferent against HCl present in the solution. The titration equations in this case can be expressed as follows:

$HCl + NaF \rightarrow HF + NaCl$ (III)

$HF + NaCl + NaOH \rightarrow H_2O + NaF + NaCl$ (IV)

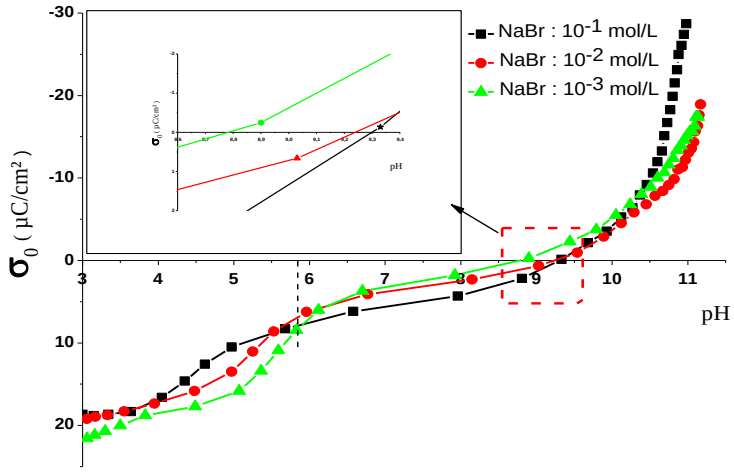

Figure 5: Potentiometric titration curves σ_0 vs pH obtained in the presence of various concentrations of a non-specific adsorption (NaBr) and 5 g/L of bentonite

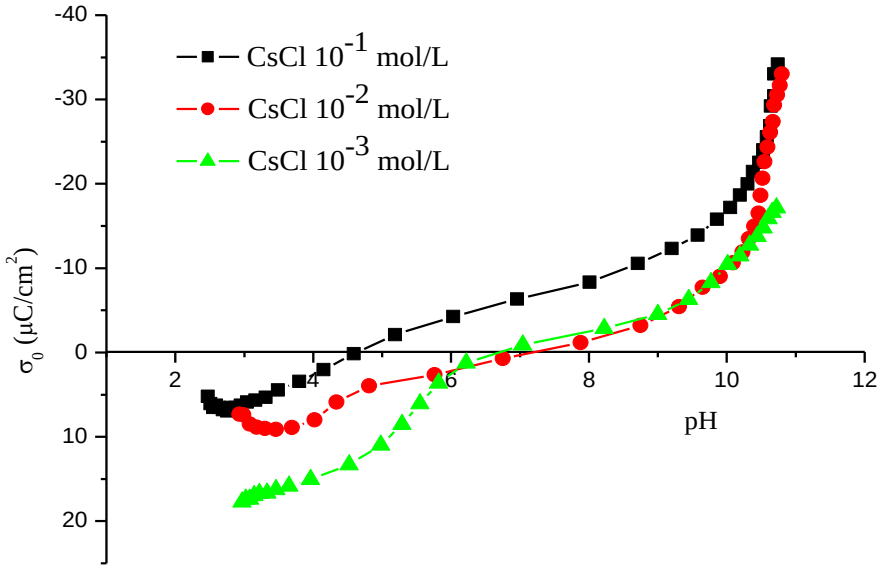

Figure 6: Potentiometric titration curves σ_0 vs pH obtained in the presence of various concentrations of a specific adsorption (CsCl) and 5 g/L of bentonite

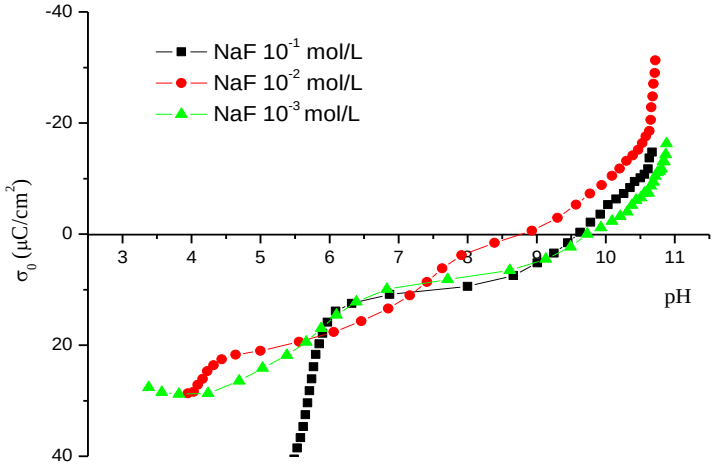

Figure 7: Potentiometric titration curves σ_0 vs pH obtained in the presence of various concentration of a specific adsorption (NaF) and 5 g/L of bentonite

3.3. Action's nature of the dispersed phase on the dispersing phase

The determination of the action's nature of the dispersed phase on the dispersing phase is essential to study the stability of a colloidal suspension. In fact, the presence of a permanent hydration layer on the particle surfaces increases considerably the stability of the studied hydrosol [52]. In this work, the adsorption studies of Li^+, Na^+ and Cs^+ cations have been carried out for pH values superior to pH_{pzc}. For pH values below the pH_{pzc}, the adsorption studies were carried out in the presence of F^-, Cl^- and Br^- anions.

Figure 8 shows the observed cationic adsorption sequence (for Cs^+, Na^+ and Li^+ cations) in the presence of bentonite samples at pH range superior to pH_{pzc}. Generally, at a given pH value, more an ion is adsorbed on a surface, more the developed surface charge density is larger. So, the observed sequence of the adsorption of the three studied cations on bentonite can be expressed as follows: $Cs^+ > Na^+ > Li^+$. An analogous study carried out at pH range below pH_{pzc} in the presence of various anionic strengths (F^-, Cl^- and Br^- anions).

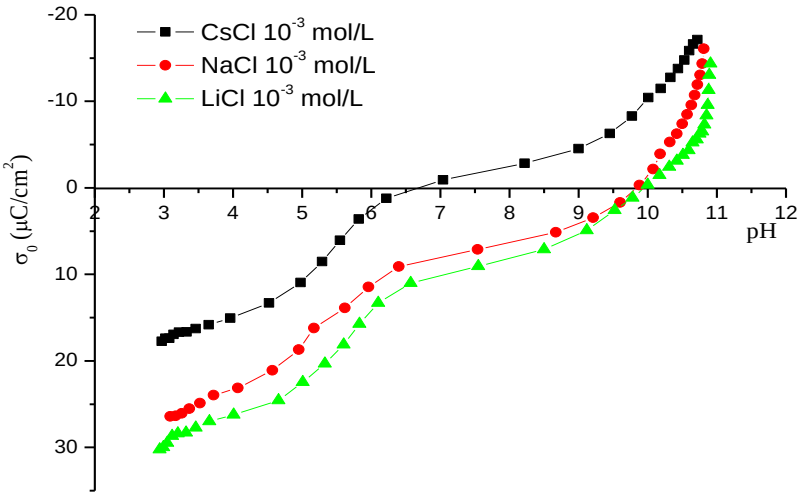

Figure 8: Cationic adsorption's sequence in the presence of bentonite samples at pH range superior to pH_{pzc}

Figure 9 shows that the anionic adsorption sequence of the three studied anions can be classified as follows:
$F^- > Cl^- > Br^-$, suggesting that F^- was more adsorbed than Cl^- and Br^- ions.

The observed sequence of the ionic adsorption on the studied bentonite samples requires the determination of the interactions between the surface of the solid and water, the surface of the solid and the ions, and between the ions and water. According to Evans, Gurney and Gierst's theoretical models [22,53,54], more an ion is adsorbed into an interface, more its action on the structure of the water is similar to that of this interface. Consequently, Cs^+,

which was the most adsorbed ion into the surface negatively charged, was classed as a structure breaker of the water [55]. In contrast, F^-, which was the most adsorbed ion on the positively charged surface, was classed as a structure promoter in aqueous solutions. Therefore, the studied natural bentonite particles in aqueous phase have a dual behavior: at pH below pH_{pzc}, they behave as a water structure organizer whereas at pH range superior to pH_{pzc}, they behave as a water structure disorganizer.

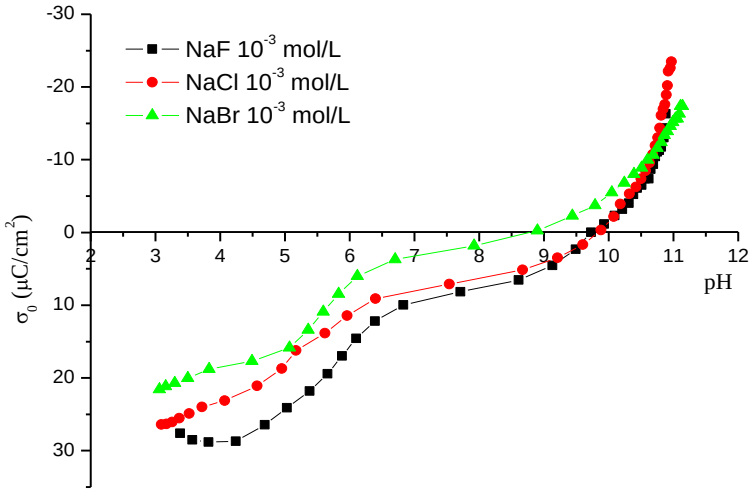

Figure 9: Anionic adsorption's sequence in the presence of bentonite samples at pH range below pH_{pzc}

3.4. Total number of surface sites

The total number of surface sites (Ns) has been determined in this work by using the graphical extrapolation method based on the application of the amphoteric sites' model reported by Stumm, Huang and Jenkins (SHJ) [28,56]. This model is based on the choice of the electrolytes depending on the action's nature of the solid in dispersing phase.

The graphic extrapolation corresponding to the F^-, which was the most adsorbed ion on the positively charged surface, determines the positively charged sites number (N_s^+), while that corresponding to the Cs^+, which was the most adsorbed ion on the negatively charged surface, gives the negatively charged sites number (N_s^-). The total sites' number is $N_s = N_s^+ + N_s^-$. Following the SHJ's model [28,56] and Huang and Stumm [57], the obtained linear equations were:

$$\frac{1}{H_s^+} = \frac{N_s^+}{\sigma_0}.\frac{1}{K_{int}^+} - \frac{1}{K_{int}^+} \qquad \text{(eq. 8)} \quad \text{for pH below } pH_{pzc}$$

And

$$H_s^+ = -\frac{N_s^-}{\sigma_0}.K_{int}^- - K_{int}^- \qquad \text{(eq. 9)} \quad \text{for pH superior to } pH_{pzc}$$

where K_{int}^+ and K_{int}^- were the intrinsic acidity constants corresponding to the positively and negatively charged surfaces, respectively.

Figures 10A and 10B show that the experimental data fitted linear plots with acceptable coefficients of determination (>0.97). N_s^- and N_s^+ calculated from the slopes and the intercepts were 97.15 and 21.13 µC/cm^2, respectively and the total density of surface sites of the bentonite was:

$$N_s = N_s^- + N_s^+ = 118.28\ \mu C/cm^2$$

To determine the maximal exchange capacity of adsorbat-adsorbent, it is necessary to convert the number Ns to the number of OH group by nm^2 of the solid, denoted D_s and defined as [58]:

$$D_s = \frac{\text{Surface sites number}}{\text{Surface unit}} = \frac{n_s.N_{Av}}{A.m_s} \qquad \text{(eq. 10)}$$

where n_s is the equivalent number of mole of titrated sites, A the surface specific area, m_s the mass of the solid and N_{Av} the Avogadro's number.

The obtained value of D_s was 6.24 10^{-2}.Ns OH/nm^2 = 7.4 OH/nm^2.

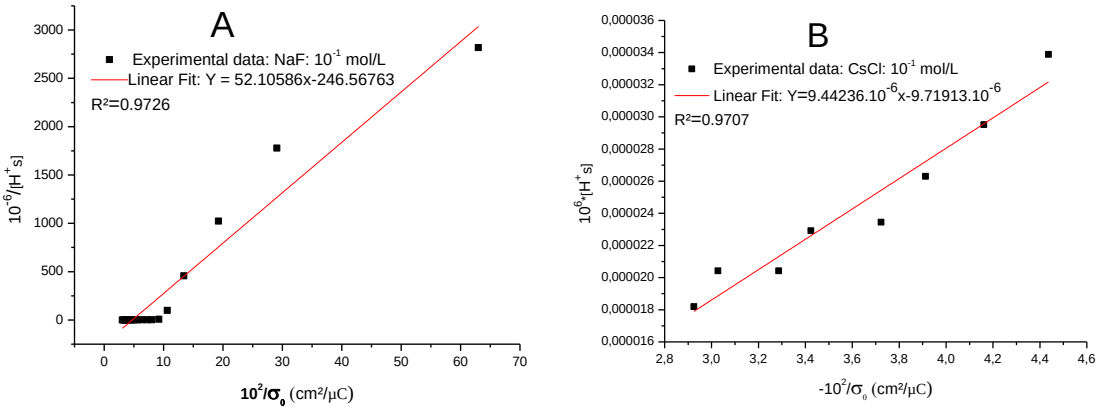

Figure 10: Determination of the total density of surface sites by using the graphical extrapolation method [28,56,59].

3.5. Ionization and complexation constants of bentonite sample

The ionization and complexation constants have been determined by applying the Davis, James and Leckie's (DJL) site-binding model [59,60].

3.5.1. Ionization constants

- In the pH range below the pH_{pzc}, the surface particles are positively charged:

$$pK_{int}^{+} = pH + \log\left(\frac{\alpha^{+}}{1-\alpha^{+}}\right) + \frac{e\Psi_0}{2.303kT} - \log\left\{1 + K_{int}^{An}[An^{-}]\exp\left(\frac{e\Psi_\beta}{2.303kT}\right)\right\} \quad \text{(eq. 11)}$$

$$pK_{int}^{+} = pQ^{+} + \frac{e\Psi_0}{2.303kT} - \log\left\{1 + K_{int}^{An}[An^{-}]\exp\left(\frac{e\Psi_\beta}{2.303kT}\right)\right\} \quad \text{(eq. 12)}$$

Where: α^{+} is the fraction of the positively charged sites

Ψ_0 ; Ψ_β are the mean potentials in the plane of surface charge σ_0 and the specifically adsorbed counter-ions σ_β, respectively

k is the Boltzman constant

T is the temperature

K_{int}^{An} is the intrinsic complexation constant surface of the anion

The pK_{int}^{+} constant can be determined by using the D.J.L's double extrapolation graphic method [59,60] ($\alpha^{+} \rightarrow 0$ and $C_s \rightarrow 0$ mol/L) of the plot of pQ^{+} vs $10\alpha^{+} + \sqrt{C_s}$.

- In the pH range above the pH_{pzc}, the surface particles are negatively charged:

$$pK_{int}^{-} = pH - \log\left(\frac{\alpha^{-}}{1-\alpha^{-}}\right) + \frac{e\Psi_0}{2.303kT} + \log\left\{1 + K_{int}^{Ca}[Ca^{+}]\exp\left(-\frac{e\Psi_\beta}{2.303kT}\right)\right\} \quad \text{(eq. 13)}$$

$$pK_{int}^{-} = pQ^{-} + \frac{e\Psi_0}{2.303kT} + \log\left\{1 + K_{int}^{Ca}[Ca^{+}]\exp\left(-\frac{e\Psi_\beta}{2.303kT}\right)\right\} \quad \text{(eq. 14)}$$

The pK_{int}^{-} constant can be determined by using the D.J.L's double extrapolation graphic method [59,60] ($\alpha^{-} \rightarrow 0$ and $C_s \rightarrow 0$ mol/L) of the plot of pQ^{-} vs $10\alpha^{-} + \sqrt{C_s}$.

The obtained pK_{int}^{+} and pK_{int}^{-} values for the aqueous suspension of bentonite in the presence of various electrolytes are presented in Table 2. It is clearly shown that $pK_{int}^{-}(Cs^{+}) < pK_{int}^{-}(Na^{+}) < pK_{int}^{-}(Li^{+})$. This observation is in good agreement with the sequence of the adsorption of these cations, early observed in the presence of the betonite samples for pH > pH_{pzc}. Table 2 shows that the obtained pK_{int}^{+} values corresponding to the non-specifically adsorption of LiCl and NaCl electrolytes were equals to 7.6. So, only the obtained pK_{int}^{+} values of F^{-}, Cl^{-} and Br^{-} ions were compared. Table 2 shows also that $pK_{int}^{+}(F^{-}) > pK_{int}^{+}(Cl^{-}) > pK_{int}^{+}(Br^{-})$. These results are in agreement with the classification of these three anions deduced from Figure 7 (F^{-} >Cl^{-}>Br^{-}) which suggested that F^{-} was more adsorbed than Cl^{-} and Br^{-} ions.

Table 2: pK_{int}^{+} and pK_{int}^{-} values for the aqueous suspension of bentonite in the presence of various electrolytes

Electrolyte	LiCl	NaCl	CsCl	NaF	NaBr
pK_{int}^{-}	12.2	11.7	9	12	11.5
pK_{int}^{+}	7.6	7.6	4.75	8.5	7

3.5.2. Complexation constants

- In the pH range below the pH_{pzc}, the surface particles are positively charged:

$$p^*K_{int}^{An} = pK_{int}^{+} - pK_{int}^{An} = pH + \log\left(\frac{\alpha^+}{1-\alpha^+}\right) - \log[An^-] + \frac{e(\Psi_0 - \Psi_\beta)}{2.303kT}$$

$$= p^*Q^{An} + \frac{e(\Psi_0 - \Psi_\beta)}{2.303kT} \qquad \text{(eq. 14)}$$

The $p^*K_{int}^{An}$ constant can be determined by using the D.J.L's double extrapolation graphic method [59,60] ($\alpha^+ \rightarrow 0$ and $C_s \rightarrow 1$ mol/L) of the plot of p^*Q^{An} according to $10\alpha^+ - \log C_s$, using the data of surface charges corresponding to high ionic forces.

- In the pH range above the pH_{pzc}, the surface particles are negatively charged:

$$p^*K_{int}^{Ca} = pK_{int}^{+} - pK_{int}^{Ca} = pH + \log\left(\frac{\alpha^-}{1-\alpha^-}\right) + \log[Ca^+] + \frac{e(\Psi_0 - \Psi_\beta)}{2.303kT}$$

$$= p^*Q^{Ca} + \frac{e(\Psi_0 - \Psi_\beta)}{2.303kT} \qquad \text{(eq. 15)}$$

The $p^*K_{int}^{Ca}$ constant can be determined by using the D.J.L's double extrapolation graphic method [59,60] ($\alpha^+ \rightarrow 0$ and $C_s \rightarrow 1$ mol/L) of the plot of p^*Q^{Ca} vs $10\alpha^- - \log C_s$, using the data of surface charges corresponding to high ionic forces. This choice was based on the Davis-James and Leckie's studies [59,61]. These authors have determined the intrinsic constants of complexation assuming that at higher electrolyte concentrations ($> 10^{-3}$ mol/L), the surface charges were essentially due to the formation of the complexes on the surface. Table 3 presents the obtained $p^*K_{int}^{Ca}$ and $p^*K_{int}^{An}$ values for the aqueous suspension of bentonite in the presence of various electrolytes

Physically, they are the K_{int}^{Ca} and K_{int}^{An} constants which express the complexation phenomenon occurring on the surface solid [62]. The similar values of $\log(K_{int}^{Ca})$ obtained for Li^+ and Na^+ (Table 3) suggest that the adsorption of these cations on the negatively charged surface of bentonite was exclusively electrostatic in nature. In contrast, the very different value of $\log(K_{int}^{Cs^+})$, compared to those of $\log(K_{int}^{Li^+})$ and $\log(K_{int}^{Na^+})$, indicates that the complexation phenomenon of the negatively charged surface by Cs^+ was both electrostatic and specific in nature. Analogously, the comparison of the obtained values of pK_{int}^{An} (Table 3) for Cl^-, Br^- and F^- anions suggests that the adsorption of Cl^- and Br^- on the positively charged surface of bentonite was exclusively electrostatic, while that of F^- was both electrostatic and specific in nature.

Table 3: $p^*K_{int}^{Ca}$ and $p^*K_{int}^{An}$ values for the aqueous suspension of bentonite in the presence of various electrolytes

Nature of electrolyte	LiCl	NaCl	CsCl	NaF	NaBr
$p^*K_{int}^{Ca}$	10.6	10.5	3.5	-	-
$p^*K_{int}^{An}$	-	7.2	-	7.5	6.8
$\log(K_{int}^{Ca}) = pK_{int}^{-} - p^*K_{int}^{Ca}$	1.6	1.2	5.5	-	-
$pK_{int}^{An} = pK_{int}^{+} - p^*K_{int}^{An}$	-	0.4	-	1	0.2

Conclusion

In this work, the interfacial electrochemical properties of a purified Moroccan bentonite sample were studied. The conductometric studies showed that the studied samples can be considered stable in aqueous phase in the studied pH range (3-12). The potentiometric titration results obtained in the presence of various concentrations of non-specifically adsorbed electrolytes showed that the point of zero charge shifted to lower pH values by increasing electrolyte concentrations. This behavior was attributed to the combined effect of both variable charges and structural negative charges. The adsorption sequence's study carried out at various ionic strengths showed that the bentonite particles in aqueous phase behave as a water structure organizer at pH below pH_{pzc}, while at pH range superior to pH_{pzc} they behave as a water structure disorganizer. The total number of surface sites was 7.4 OH/nm^2. The analysis of the obtained complexation constant values corresponding to the non-specifically adsorbed ions showed that their adsorption mechanism on the solid was exclusively electrostatic in nature. In contrast, the specific adsorption of ions was both electrostatic and specific in nature.

References

1. Bilgiç C., *J. Colloid Interf. Sci*. 281 (2005) 33-38.
2. Tahir S.S., Naseem R., *Sep. Purif. Technol*. 53 (2007) 312–321.
3. Eren E., Afsin B., *J. Hazard. Mater*., 151 (2008) 682–691.
4. Demirbas A., Sari A., Isildak O., *J. Hazard. Mater*. 135 (2006) 226–231.
5. Bojemueller E., Nennemann A., Lagaly G., *Appl. Clay Sci.* 18 (2001) 277–284.
6. Bors J., Dultz S., Riebe B., *Appl. Clay Sci.* 16 (2000) 1–13.
7. Ddani M., Meunier A., Zahraoui M., Beaufort D., El Wartiti M., Fontaine C., Boukili B., El Mahi B., *Clays Clay Miner*. 53 (2005) 250-267.
8. Bergaya F., Theng B.K.G., Lagaly G., Development in Clay Science, Handbook of Clay Science, Elsevier, volume 1 (2006) 1-1224
9. Madejova J., *Vib. Spectrosc*. 31 (2003)1-10.
10. Güven N., Pollastro R.M., Clay-Water Interface and its Rheological Implications, The clay Minerals Society, Boulder, CO, USA (1992).
11. Velde B., Origin and Mineralogy of Clays: Clays and the Environment, Springer-Verlag (1995).
12. Mc Bride M.B., Minerals in Soil Environments, Soil Science Society America, (1989).
13. Borchardt G., Minerals in Soil Environments, Soil Science Society of America, (1989).
14. Bleam W.F., Welhouse G.J., Janowiak MA., *Clays Clay Miner*. 41 (1993) 305-316.
15. Bleam W.F., *Clays Clay Miner*. 38 (1990) 527-536.
16. Avena M.J., Cabrol R., Pauli C.P. *Clay clay Miner*. 38 (1990) 356-362.
17. Avena M.J., Pauli C.P. *J. Colloid InterfaceSci*. 202 (1998)195-204.
18. Missana T., Adell A. *J. Colloid Interface Sci*. 230 (2000)150-156.
19. Leroy P., Revil A. *J. Colloid Interface Sci*. 270 (2004)371-380.
20. Baeyens B., Bradbury M.H. *J.Contam. Hydrol*. 27 (1997)199-222.
21. Wanner H., Albinsson Y., Karnland O., Wieland E., Wersin P., Charlet L. *Radiochim. Acta*. 66/67 (1994) 157-162.
22. Lützenkirchen J., *J. Colloid Interf. Sci*. 290 (2005) 489-497..
23. Lützenkirchen J., Boily J.F., Lövgren L., Sjöberg S. *Geochim. Cosmochim. Acta*. 66 (2002) 3389-3396.
24. Du Q., Sun Z., Forsling W., Tang H., *J. Colloid Interf. Sci*. 187 (1997) 221-231.
25. Avena M.J., Pauli C.P., *Colloids Surfaces A: Physicochem. Eng. Asp*. 118 (1996) 75-87.
26. Duc M., Gaboriaud F., Thomas F., *J. Colloid Interface Sci*. 289 (2005)148-156.
27. Duc M., Gaboriaud F., Thomas F., *J. Colloid Interface Sci*. 289 (2005) 139-147
28. Huang C.P., Stumm W., *J. Colloid Interface Sci*. 43 (1973) 409-420.
29. HiemstraT., Wit J.C.M., Van Riemsdijk W.H., *J. Colloid Interface Sci*. 133 (1989)105-117.
30. Duc M., Thomas F., Gaboriaud F., *J. Colloid Interface Sci*. 300 (2006) 616-625.
31. Daou I., Zegaoui O., Chfaira R., Ahlafi H., Moussout H., *Int. J. Sci. Res. Publ*. 5 (2015) 293-301.
32. Metz V., Amram K., Ganor J., *Geochim Cosmochim Acta*. 69 (2005)1755-1772.
33. Daou I., Chfaira R., Zegaoui O., Aouni Z., Ahlafi H., *Mediterr. J. Chem*. 2 (2013) 569-582.
34. Sposito G. The Chemistry of Soils, 2nd , Oxford Unversity press, (2008)
35. Sparks D.L. Environmental Soil Chemistry, 2nd, Academic Press San Diego, (2003).
36. Morais F.I., Page A.L., Lund L.J., *Soil Sci. Soc. Am. J*. 40 (1976) 521-527.
37. Bouby M., Lützenkirchen J., Dardenne K., Preocanin T., Denecke M.A., Klenze R., Geckeis H., *J. Colloid Interface Sci*. 350 (2010) 551-561.
38. Kosmulski M., *J. Colloid Interface Sci*. 353 (2011) 1-15.
39. Appel C., Ma L.Q., Rhue R.D., Kennelley E., *Geoderma*. 113 (2003) 77-93.
40. Chorover J., Sposito G., *Geochim. Cosmochim. Acta*. 59 (1995) 875-884.
41. Phillips I.R., Sheehan K.J., *Aus. J. Soil. Res*. 43 (2005) 915-927.
42. Zelazny L., He W., Vanwormhoudt L. Charge Analyses of Soils and Anion Exchange, Soil Science Society of America, (1996).
43. Chang F.R.C., Sposito G., *J. Colloid Interface Sci*. 163 (1994) 19-27.
44. Avena M.J., Mariscal M.M., Pauli C.P., *Appl. Clay Sci*. 24 (2003) 3-9.
45. Kraepiel A.M.L., Keller K., Morel F.M.M., *J. Colloid Interface Sci*. 210 (1999) 43-54.
46. Madrid L., Diazbarrientos E. *J. Soil Sci*. 39 (1988) 215-225.
47. Hendershot W.H., Lavkulich L.M. *Soil Sci. Soc. Am. J*. 47 (1983) 1252-1260.

48. Van Raij B., Peech M., *Soil Sci. Soc. Am. proc*. 36 (1972) 587-593.
49. Laverdière M.R., Weaver R.M., *Soil Sci. Soc.Am. J*. 41 (1977) 505-510.
50. Polubesova T.A., Chorover J., Sposito G., *Soil Sci. Soc. Am. J*. 59 (1995) 772-777
51. Cao E., Bryant R., Williams D.J.A., *J. Colloid Interface Sci*. 179 (1996)143-150.
52. Erkov V.G., Devyatova S., Molodstova E.L., Malsteva T.V., Yanovskii U.A., *Appl. Surf. Sci*. 166 (2000) 51-56
53. Dumont F., Verbeiren P., Buess-Herman C., *Colloids Surfaces A:Physicochem. Eng. Asp*. 149 (1999) 149-156.
54. Piasecki W., Zarzycki P., Charmas R., *Adsorption* 16(2010) 295-303.
55. Lyklema J., *Chem. Phys. Lett*. 467 (2009) 217-222..
56. Stumm W., Chemistry of the Solid-Water Interface: Processes at the Mineral- Water and Particle-Water Interface in Natural Systems. New York: Wiley Interscience Pub; (1992).
57. Davis J.A., Leckie J.O., *J. Colloid Interface Sci*. 67 (1978) 90-107.
58. Boisvert J., Malgat A., Pochard I., Daneault C., *Polymer (Guildf)*. 43 (2002)141-148.
59. Waychunas G.A., Fuller C.C., Davis J.A., *Geochim.Cosmochim. Acta*. 66 (2002) 1119-1137.
60. Payne T.E., Davis J.A., Lumpkin G.R., Chisari R., Waite T. D., *Appl. Clay Sci*. 26 (2004) 151-162.
61. Malgat A, Boisvert J, Daneault C., *J. Colloid Interface Sci*. 269 (2004) 320-328.
62. Hunter R.J., Clarendon Press, Oxford University Press, 1 (1987) 379-391.

(2017) ; http://www.jmaterenvironsci.com